

Design and optimization of cyclized NK₁ antagonists with controlled atropisomeric properties

Jeffrey S. Albert,^{*} Cyrus Ohnmacht, Peter R. Bernstein, William L. Rumsey,[†] David Aharony, Brian B. Masek,[‡] Bruce T. Dembofsky, Gerard M. Koether, William Potts and John L. Evenden

CNS Discovery Research, AstraZeneca Pharmaceuticals LP, 1800 Concord Pike, PO Box 15437, Wilmington, DE 19850-5437, USA

Received 10 October 2003; revised 12 March 2004; accepted 19 March 2004

Abstract—We have previously described a series of antagonists that showed high potency and selectivity for the NK₁ receptor. However, these compounds also had the undesirable property of existing as a mixture of four interconverting rotational isomers. Through biological and structural analysis of the atropisomers, a binding model was developed and used to guide the design of compounds, which were rigidified by installation of a cyclizing linkage. These compounds existed as a mixture of two atropisomers. Further elaboration of the ring system reinforced the desired conformation and eliminated atropisomeric properties. We found that the region distal to the 8-membered ring system could be modified while retaining NK₁ potency, and optimization led to further improvements in the *in vivo* activity.

© 2004 Elsevier Ltd. All rights reserved.

1. Introduction

The tachykinins are a family of three mammalian neuropeptides: substance P (SP), neurokinin A (NKA), and neurokinin B (NKB). The preferred receptors for these are termed NK₁, NK₂ and NK₃, respectively. Substance P is widely distributed in the CNS and peripheral tissue and acts as a neurotransmitter or neuro-modulatory agent. The NK₁ receptor may be involved in several pathophysiological conditions including asthma, emesis, anxiety, depression, and pain.^{1,2} The discovery of tachykinin antagonists has been extensively reviewed.^{3–6}

Since the identification of the first non-peptidic tachykinin

antagonist CP-96,345,⁷ the area has received intense interest. This reflects the potential clinical importance that tachykinin antagonists are viewed to have. Prompted by the identification of the NK₂ antagonist SR-48,968,⁸ our group initiated a program to identify NK₁ and NK₂ antagonists. These efforts led to the discovery of **1** (Fig. 1). As a result of the naphthyl 2-substituent, this compound was more than two log units more potent as an NK₁ antagonist than as an NK₂ antagonist (pK_B 9.6 vs. 7.3, respectively). This compound was advanced for the treatment of depression.⁹

Compound **1** has two bonds with restricted rotation. The amide bond can exist in the *s-cis* or *s-trans* forms, and the carbonyl–aryl bond can exist in the *S*-axial or *R*-axial

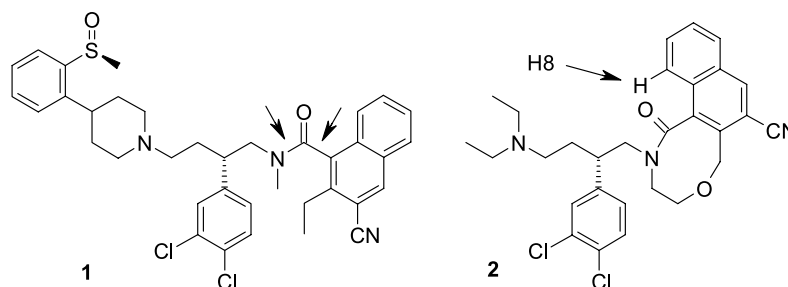


Figure 1. Left: structure of **1**, arrows indicate bonds with restricted rotation. Right: structure of **2**, arrow indicates the naphthalene H8.

Keywords: Tachykinin; Neurokinin; Atropisomer.

^{*} Corresponding author. Tel.: +1-302-886-4771; e-mail address: jeffrey.albert@astrazeneca.com

[†] Present address: GlaxoSmithKline, 709 Swedeland Rd, UW2532, PO Box 1539, King of Prussia, PA 19406-0939, USA.

[‡] Present address: Optive Research, Inc., 7000 North Mopac Expressway, Austin, TX 78731, USA.

configurations. The barrier to rotation is sufficiently high such that four atropisomers (interconverting rotational isomers) can clearly be seen by HPLC (Fig. 2) and NMR spectroscopy.

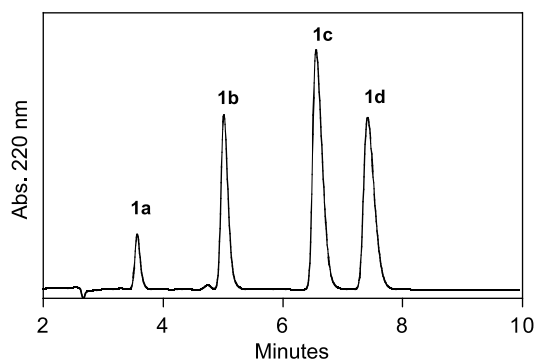


Figure 2. High pressure liquid chromatogram (HPLC) of **1** showing the resolution of the atropisomeric forms (**1a–1d**). Conditions: column; Phenomenex Luna C18(2) 3 μ m, 4.6 \times 75 mm; 60% methanol, 40% water (0.1% TFA), 1.5 mL/min. UV detection at 220 nM.

For a candidate drug, equilibrating atropisomeric properties would present possible safety concerns as well as very substantial complications for manufacturing and analytical development. To better understand the properties of **1**, we purified and independently studied each of the atropisomers (designated **1a**, **1b**, **1c**, and **1d**) by preparative HPLC. We observed that interconversion occurred primarily between atropisomers **1a/1d** and between **1b/1c**; interconversion between all other pairs (i.e. **1d/1b**, **1b/1a**, **1a/1c**, and **1c/1d**) was not seen.¹⁰ Such behavior has been observed for related naphthamide systems.¹¹ In these cases, it is understood that the fastest interconversions are due to the simultaneous, paired rotation of the naphthamide–aryl and amide bonds.^{11,12} This occurs because steric strain develops as the naphthamide or amide undergoes rotation; as a result, the rotations must occur together. This process is referred to as ‘gated rotation.’¹³

The long rotational half-life (approximately 1.8 days at 37 °C) allowed us to individually test each component of **1**.¹⁰ We found that most of the *in vivo* NK₁ activity was associated with the single atropisomer, **1d**. Using a combination of kinetic and spectroscopic studies, we assigned structures for each of the atropisomers as indicated in Figure 3.¹⁰

Based on the structural model for **1d**, we reasoned that we could enforce the single, desired conformation by introducing a tether to connect the methyl group of the amide with the naphthalene 2-position. Such a tether should stabilize the NK₁ binding conformation because the amide would be locked in the *trans* configuration. A similar approach has been demonstrated for a structurally unrelated series of NK₁ antagonists.¹⁴

We analyzed compounds with tethering ring systems containing 6, 7, and 8-membered rings and found that the 8-membered ring system was preferred.¹⁵ Prior studies had shown that the piperidine substituent in **1** could be simplified¹⁵ without significant loss of NK₁ receptor

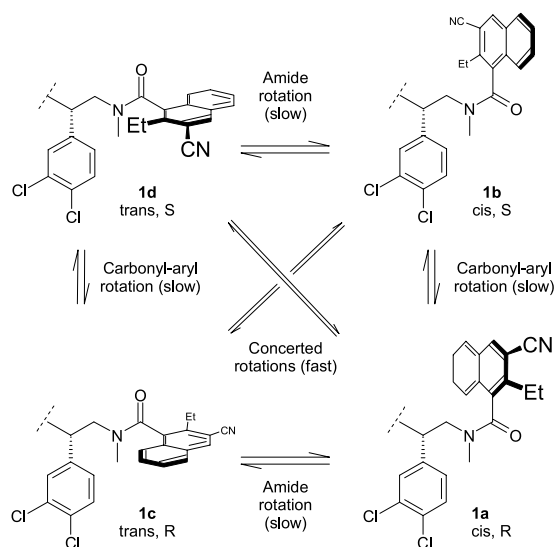


Figure 3. Model for the interconversion path and structural assignments for atropisomers **1a–1d**.

antagonist potency. Combining the 8-membered ring with the simplified piperidine led to the identification of **2**;¹⁵ this compound maintained high NK₁ potency and selectivity (Table 1). As expected, conformational properties are simplified for compound **2** as a result of the cyclizing tether; it exists as a mixture of only two atropisomers which are presumably the *R*- and *S*-axial carbonyl-naphthalene isomers.

Table 1. NK₁ Receptor antagonist potency (pK_B) for **1** and **2**^a

Compound	NK ₁ ^b	NK ₂ ^c
1	9.56 \pm 0.04	7.31 \pm 0.28
2	9.50 \pm 0.14	<7

^a pK_B Determinations using rabbit pulmonary artery tissue ($n=2-6$).

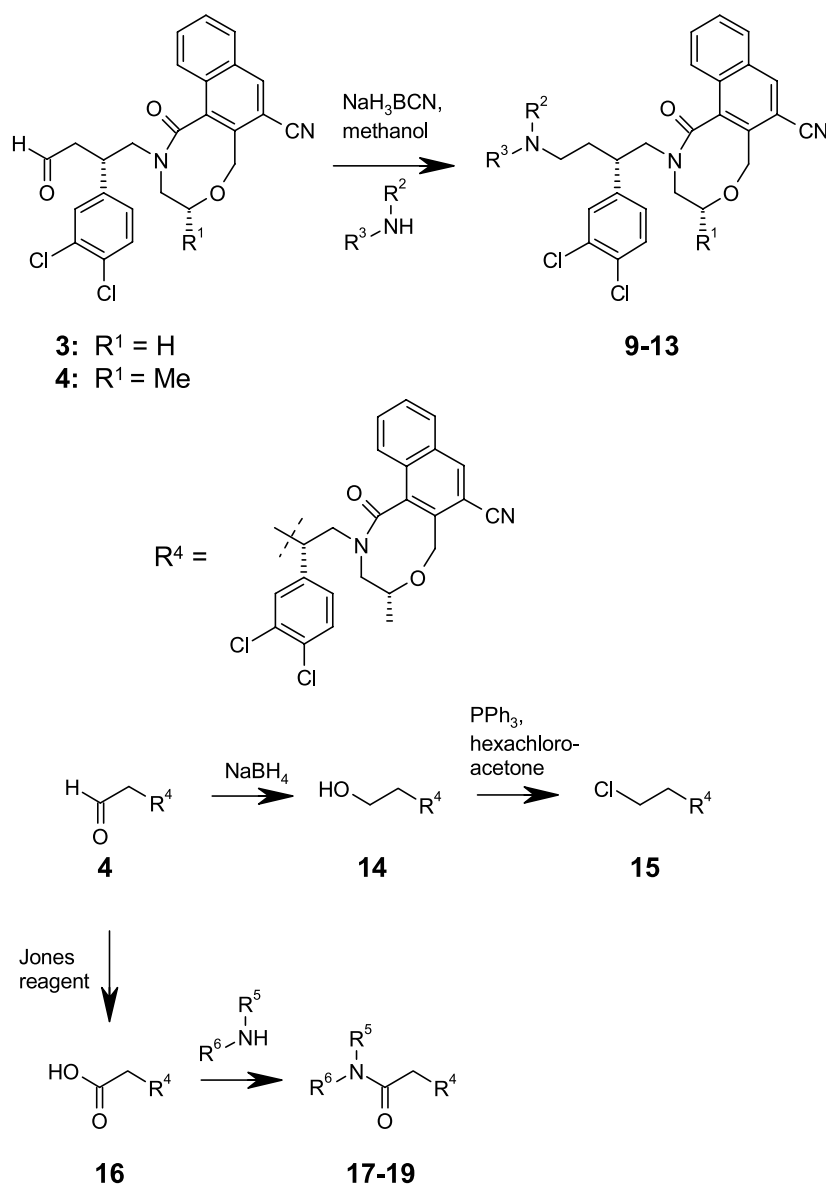
^b Agonist: Ac-(Arg⁶, Sar⁹, Met(O₂)¹¹) SP₆₋₁₁ (ASMSP).

^c Agonist: BANK (β -ala⁸NKA(4-10)).

After demonstrating that we could reduce the number of isomers from four to two, our next goal became the stabilization of a single conformation. In this way, all potential concerns about atropisomerism would be eliminated. This paper describes the modeling and structural analysis of these 8-membered ring antagonists. In these studies, we have developed a series of novel NK₁ antagonists that exist in predominantly a single conformation. Furthermore, by comparing these compounds, we have constructed a detailed pharmacophore model for NK₁ receptor binding.

2. Synthesis

Secondary and tertiary amine compounds could be conveniently prepared from aldehyde **3**¹⁵ or **4**¹⁵ by reductive amination in the presence of sodium cyanoborohydride. Alcohol and carboxylic acid derived compounds were prepared by reduction or oxidation of **4** as indicated in the Scheme 1.



Scheme 1. For R², R³, R⁵, R⁶ see Table 4.

3. Results

To better understand the factors responsible for the atropisomeric properties, molecular modeling studies were conducted for the cyclic analogs. With **2** as a starting point, and with knowledge of the rotational properties of related naphthamides, we sought to eliminate the atropisomeric properties. A detailed analysis of the ground state energetics was carried out for compounds in the cyclic series to explore this possibility.

3.1. Conformational analysis of the 8-membered ring system

To more fully understand the conformational properties of **2** and related compounds, we began by considering simpler model systems. Analysis of the possible conformations of the 8-membered ring was carried out by first considering 1,3-cyclo-octadiene (COD) (Fig. 4). As a first approximation, the *cis* double bonds in COD are expected to

constrain the torsional angles in the 8-membered ring in a manner similar to that for the aryl and amide bonds in **2**. Thus, COD serves as a convenient starting point because its conformational properties have been extensively studied,^{16–19} both theoretically and experimentally.

Previous studies indicate three relevant conformations for COD, a twist boat chair (TBC) conformation, and the two twist boats (TB1 and TB2) conformations (Fig. 5). We began by verifying that the conformational energetics calculated by our AESOP-Enigma program²⁰ were quantitatively consistent with empirical data and with energies determined by other theoretical methods. Next, we examined the energetics of these same conformations in the more elaborate cyanobenzamide and cyanonaphthamide-based ring systems (Fig. 5). The TBC conformers remained the most stable for both the cyanobenzamide and cyanonaphthamide adducts. Interestingly, both TB1 and TB2 conformers are substantially destabilized in these systems relative to COD. It is important to note that

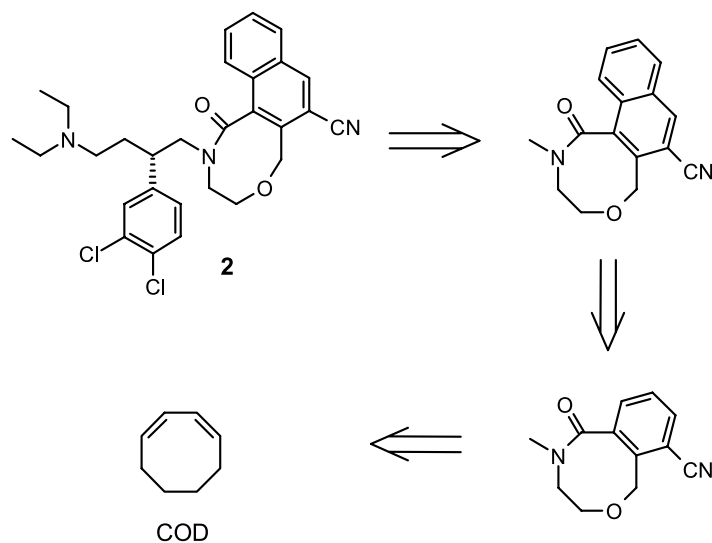


Figure 4. Progressive simplification from the 8-membered ring system in **2** to the simplified naphthalene analog, to the simplified benzamide analog, to COD.

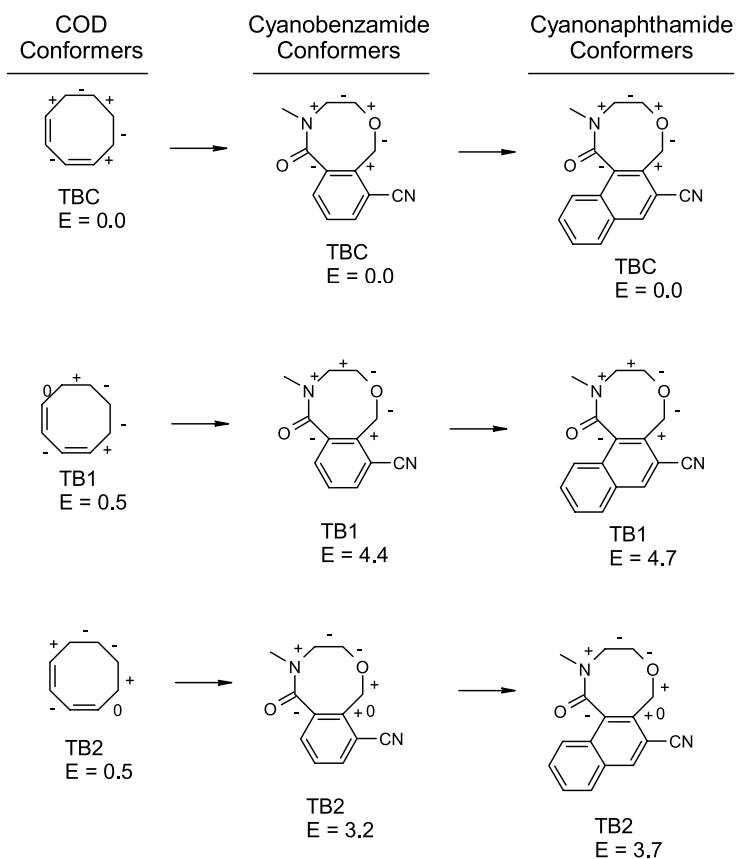


Figure 5. Relative conformational energies (kcal/mol) for COD, and cyanobenzamide and cyanonaphthamide model systems. The sign of the torsional angles for each bond in the 8-membered ring are indicated with (-) and (+).

all three conformations (TBC, TB1 and TB2) are chiral; a corresponding enantiomeric conformation exists for each of these conformations. (The enantiomeric conformation has an inversion of the sign of each of the torsional angles.) These pairs of enantiomeric conformations (denoted A and B below) are energetically equivalent in an achiral environment.

3.2. Conformational analysis including the pendant phenethyl side chain

As the next step in progressively elaborating from our simple starting model, a pendant phenethyl group (Fig. 6) was added to model the dichloroaryl region of compound **2**. Because the phenethyl group contains a chiral atom of

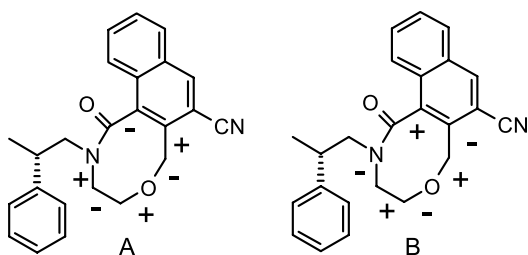


Figure 6. TBC conformations of the naphthamide system with pendant chiral phenyl containing side chain used for computational analysis. The two structures differ by inversion of the torsion angles around each atom in the 8-membered ring; the sign of the torsional angles for each bond in the 8-membered ring are indicated with (-) and (+).

known fixed absolute stereochemistry, the (previously enantiomeric) conformers of the 8-membered ring become diastereomeric and thus both forms must be considered (Fig. 6). Prior studies had shown that NK₁ and NK₂ affinity are sensitive to the stereochemistry of the aryl methine carbon, with the *S*-enantiomer being preferred.²¹ Therefore, all subsequent experimental and computational studies focused on this form.

For each ring conformation (2 TBC, 2 TB1 and 2 TB2) exhaustive conformational scanning of the pendant side chain was performed using Enigma-ConfScan.²⁰ The phenyl side chain does not appear to perturb the conformational preferences of the 8-membered ring; the conformations containing TB1 or TB2 ring conformations remained 3–4 kcal/mol higher in energy than those containing TBC conformations for the 8-membered ring system. Two conformers were found to be very close in energy; they are designated as A and B (Fig. 7). These conformers are based on TBC ring geometries of ‘opposite’ chirality as well as differing side chain geometries. The A conformer was favored by 0.7 kcal/mol over the B conformer. From this we conclude that the actual energies should be close to each other; the small predicted energy difference is within the uncertainty of the calculation.

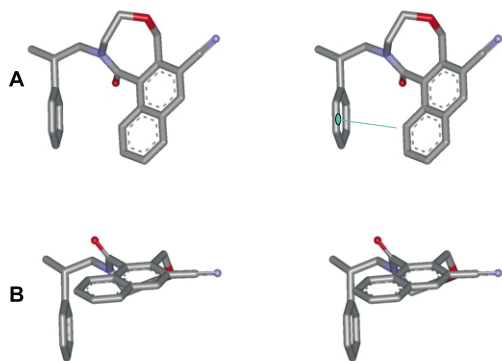


Figure 7. Relaxed-eye stereoview representation of the two low energy conformers of the model compounds from Figure 6. Conformation A shows an edge-to-face aryl–aryl stacking interaction (green line) which is hypothesized in the NK₁-active atropisomer. Conformation B cannot accommodate the stacking interaction and is hypothesized to be the less active atropisomer. Hydrogen atoms have been omitted for clarity.

3.3. Structural assignments of the 8-membered ring system

Experimentally, we observe two atropisomers for **2** with a population distribution of about 1:2 according to HPLC and ¹H NMR spectroscopy (Fig. 8). This implies that the conformational energies must be similar. For **2**, NMR spectra show that each of the two atropisomers are resolved for many of the protons. However, the separation of the corresponding signals is particularly striking for the naphthalene H8 proton. For the minor atropisomer, the naphthalene H8 proton is in the expected region at about 7.4 ppm. (It is obscured by overlapping signals but can be identified in two dimensional NMR experiments). For the major atropisomer, the naphthalene H8 proton is shifted upfield to about 6.4 ppm.

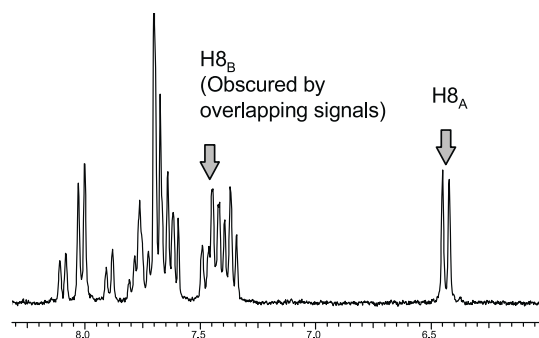


Figure 8. ¹H NMR spectrum of **2** in d₆-DMSO.

In ¹H NMR spectra of **2**, an upfield shift might be expected for the ring conformer A because the H8 proton is oriented into the shielding region of the phenyl ring (Fig. 7). For the B conformation, the H8 proton is distant from the phenyl ring, and no shift would be expected. The phenethyl side chain does not appear to perturb the conformational preferences of the 8-membered ring; conformational scanning indicated that for B, no stable conformation exists (<3 kcal/mol) for the pendant phenyl ring which would allow interaction of the naphthalene H8 proton. The atropisomeric distribution and NMR spectroscopic properties of **2** are fully consistent with the structures and energies predicted by modeling. Based on this evidence, we assigned conformations to the atropisomers as indicated in Figure 7.

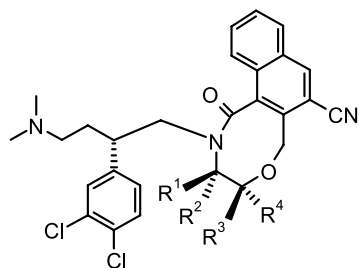
Prior studies on **1** demonstrated that it was atropisomer **1d** which was preferred for NK₁ antagonism¹⁰ (Fig. 3). The conformation of **1d** overlays well with conformer A of the 8-membered system. In particular, they share the same orientation of the amide and naphthalene–carbonyl bonds, and they both have a potential aryl–aryl stacking interaction between the dichloroaryl ring and the naphthalene ring. For these reasons, we assign conformer A as the NK₁ preferring analogue.

3.4. Rigidification of the 8-membered ring by additional substitution

Despite the potent *in vitro* activity observed for **2** (Table 1) its existence as a mixture of two atropisomers limited further consideration of this compound for drug development. Kinetic analysis showed that the interconversion

half-life between the two atropisomers was 9.7 h (37 °C, 50% acetonitrile/water, 25 mM phosphate, pH 7.0; data not shown). This rate is fast enough that it would be impractical to isolate and administer the compound as a single atropisomer. We sought to eliminate the atropisomeric properties while further improving potency.

We speculated that addition of a methyl substituent in the 8-membered ring might perturb the energies enough to stabilize one conformer with respect to the other conformer.¹⁴ Building upon the computational analysis described above, we analyzed the energies of each of the methyl substituted analogs in Figure 9. These modeling studies were used to aid conformational analysis; we have not attempted to extend the analysis for the interpretation of in vivo results which would require the addition of parameters to account for distribution, metabolism and other factors. In each of the examples, we found two predicted low energy conformers of the 8-membered ring system, which were analogous to the A and B conformations of the unsubstituted case. However, the predicted energy differences between the A and B conformers were small. Therefore, we could not reliably predict which position for substitution would most optimally stabilize the desired A-type conformation.



- 5:** R¹, R², R³, R⁴ = H
6: R¹ = Me, R², R³, R⁴ = H
7: R² = Me, R¹, R³, R⁴ = H
8: R³ = Me, R¹, R², R⁴ = H
9: R⁴ = Me, R¹, R², R³ = H

Figure 9. Structures of 5–9.

Each of the four methyl substituted analogs 6–9 were prepared and the atropisomeric distributions were analyzed by HPLC. As described above, the NK₁-preferential conformers of 1 and 2 showed a characteristic upfield shift in NMR spectra for the naphthalene H8 proton. We interpret this shift as resulting from an aryl–aryl interaction when the compound adopts a conformation like that shown in Figure 7(A). Therefore, we expected that the NK₁ preferred conformers in 6–9 would show a similar upfield shift for the naphthalene H8 proton. We determined which peaks in the HPLC chromatograms corresponded to the H8-shifted and non-shifted conformations by analysis of NMR integrations and comparison with HPLC integrations (Table 2). By extension of this, we assigned the one with the upfield shifted H8 resonance as the NK₁ preferred conformer. This assumption allowed us to expedite compound evaluation by avoiding the need to separate and test each atropisomer for each compound.

Table 2. Inhibition of ASMSp-induced foot tapping response in gerbil and receptor antagonist potency (pK_B) in rabbit pulmonary artery tissue

	pK _B ^a	% Inhibition of GFT response ^b	Isomer distribution; shifted/unshifted ^c
5	9.10±0.03	38±11	68:32
6	8.63±0.13	3±1	>98:2
7	8.64±0.09	8±3	10:90
8	8.29±0.15	23±13	31:68
9	8.34±0.24	63±23	>98:2

^a pK_B Determinations using RPA tissue (n=2–6), agonist: ASMSp.

^b Determined 4 h after oral dosing of antagonist at 5 μmol/kg and initiated by CNS administration of ASMSp (100 pmol).

^c Isomer distribution determined by HPLC. Assignments ('shifted' and 'unshifted') refer to the position of the naphthalene H8 signal in NMR spectra.

For 5–9, the distribution and assignment (H8-shifted and non-shifted) of the conformational forms are indicated in Table 2. It was evident that 7 and 8 existed as a mixture of atropisomers, and the conformational equilibrium favored the H8-nonshifted (and hence NK₁ non-preferred) conformation. In comparison, 6 and 9 existed predominantly as a single atropisomer in the H8 shifted conformation.

Detailed characterization of the four isomers will be presented separately, but key observations are summarized here. Central administration of ASMSp to gerbils induces a foot tapping (GFT) response which can be attenuated by prior dosing with an orally available CNS-penetrant, NK₁ receptor antagonist. This can provide a convenient way to assess potency of NK₁ receptor antagonists.²² Gerbils were orally treated with antagonist at 5 μmol/kg at 4 or 6 h prior to administration of agonist. The CNS potency was then quantified by comparing the foot tapping response with control animals with vehicle only. Among the four isomers, compound 9 was the most potent in the GFT model (Table 2). Furthermore, it was more potent than the unsubstituted 5. We were fortunate that this was one of the two compounds to exist as a single atropisomer; this could not have been predicted a priori.

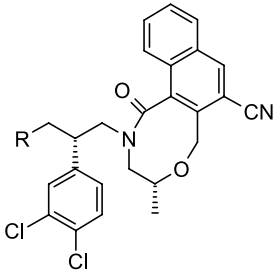
Pharmacological activity was further assessed in vitro using pulmonary artery isolated from rabbit (RPA). Rabbit neurokinin receptors are homologous to human. It is noteworthy that while 9 is the most potent isomer in the in vivo model, it does not show the highest potency (pK_B) in the in vitro functional model. While each of the methyl-substituted isomers have similar RPA potencies (pK_B 8.3–8.6), the potency is clearly greater for 5 (pK_B 9.1). Obviously, receptor binding results from multiple interactions, and it is likely that addition of the methyl groups in 6–9 introduces some unfavorable interactions in addition to altering the atropisomeric distribution. The apparent discrepancy between the in vivo and in vitro potency for 5 and 9 cannot be attributed to overall drug exposure since gerbil dose-normalized exposure levels in brain are similar between 5 (1478 ng/g following 100 μmol/kg oral dose) and 9 (224 ng/g following 30 μmol/kg oral dose).²³ Possible explanations include differences between the rabbit and gerbil receptors, or differences in exposure levels at specific brain regions. Pharmacokinetic parameters for 9 are shown in Table 3.

Table 3. Pharmacokinetic analysis of **9** in rat ($n=2$)

Pharmacokinetic parameter	Result
Oral dose ($\mu\text{mol/kg}$)	20
Formulation	75% PEG/Saline
C_{max} (nM)	265
T_{max} (h)	7
AUC-PO(0-i) (ng h/mL)	2370
Bioavailability (%)	25

3.5. Optimization of compounds based on the ring structure in **9**

Compound **9** had excellent potency in the gerbil in vivo model and existed in predominantly a single conformational form. Based on this, we sought to further increase potency in compounds containing the same 8-membered ring system. We surveyed analogs of **9** in which the ‘left side’ dimethyl amine group was replaced with groups of varying properties (Table 4). We observed that antagonist potency (pK_B) was not greatly affected over the range of substituent groups, which included basic, acidic, hydrophobic, and polar functionality. Additionally, we found that antagonist in vitro potency (pK_B) did not directly correlate with in vivo potency in the GFT model; this most likely reflects substantial differences in distribution and metabolism. For example, **9** had much greater potency than **11** in the in vivo GFT model (63% vs 3% inhibition at 4 h); whereas **9** had weaker potency than **11** in the in vitro model (pK_B 8.2 vs 9.0). The most active compound identified was **13**. It showed excellent potency with a very long duration of action (81% inhibition of response after 6 h).

Table 4. In vitro potency (pK_B) in RPA and inhibition of ASMSP-induced foot tapping response in gerbil


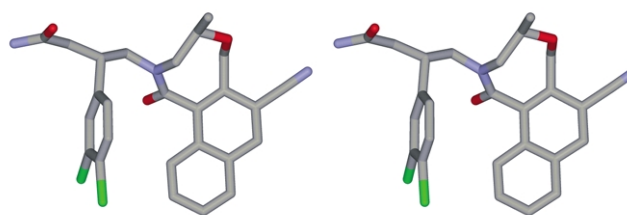
	R	pK_B^a	GFT, 4 h ^b	GFT, 6 h ^b
9	Me ₂ NCH ₂ –	8.3±0.1	63±23	52±24
10	MeNH–	9.3±0.1	5±8	9±8
11	(<i>N</i> -Piperidinyl)–CH ₂ –	9.0±0.1	3±1	3±2
12	Me ₃ CNCH ₂ –	7.8±0.1	1±0.6	38±31
13	MeONHCH ₂ –	8.2±0.1	73±6	81±19
14	HOCH ₂ –	8.6±0.3	15±7	6±3
15	ClCH ₂ –	7.9±0.1	35±5	63±13
16	HOC(O)–	8.2±0.2	1±0.3	1±0.8
17	H ₂ NC(O)–	8.8±0.1	4±2	3±1
18	MeNHC(O)–	9.0±0.3	4±2	4±2
19	Me ₂ NC(O)–	8.2±0.3	17±12	38±31

^a pK_B Determinations using rabbit pulmonary artery (RPA) tissue ($n=2-6$), agonist: ASMSP.

^b % Inhibition of gerbil foot tap (GFT) response determined after oral dosing of antagonist at 5 $\mu\text{mol/kg}$ at 4 or 6 h (as indicated) prior to initiation by CNS administration of ASMSP (100 pmol).

3.6. Structural analysis and pharmacophore model for **13**

Unfortunately, we were unable to crystallize **13**, however; we succeeded for the analog **17** (Fig. 10). Crystallographic analysis showed excellent correspondence with the assigned structure for the NK₁-preferential atropisomer **1d** (Fig. 3) and modeling of the 8-membered ring system (Fig. 7). In particular, the crystal structure shows the 8-membered ring adopting the TBC configuration with the naphthalene oriented such that the H8 proton is 3.1 Å from the dichloroaryl ring centroid. This close proximity is consistent with the upfield shift observed for this proton in NMR spectroscopy. Based on the potent in vivo activity and the structural information, we propose an NK₁ pharmacophore model involving an edge-to-face aryl–aryl stacking interaction and a polar group served by the amide carbonyl in the 8-membered ring system. The exocyclic methyl group may serve to stabilize the desired conformational form, but may also introduce penalizing interactions with the NK₁ receptor. Finally, we note that there is substantial tolerance to substitution at the left-side region in this series which could therefore be used to further optimize distribution and metabolic properties.

**Figure 10.** Crystal structure of **17**. The dichloroaryl ring exists both in the orientation shown, and with rotation such that 3-chloro group is on the ‘alternate’ 3-carbon. The structure is shown as a relaxed-eye stereoview with hydrogen atoms omitted for clarity.

4. Summary and conclusions

In earlier work, we developed a series of potent and selective NK₁ antagonists. However, this series had the undesirable property of existing as a mixture of four atropisomers. Structural analysis and comparisons of the activities of these atropisomers allowed us to construct an NK₁ pharmacophore model. This binding model was then used to design a new series in which the naphthalene amide system was constrained through a tether, thus forming an 8-membered ring. As a result of this constraint, the conformational features were simplified, and resulting compounds existed as a mixture of only two atropisomers. Through detailed computational analysis we constructed a model for both atropisomers and assigned a structure for the active conformer. In the conformational mixture, we found the NK₁ preferred component had a characteristic shift in the H8 naphthalene proton in NMR spectroscopy. The shift was suggestive of the orientation of the naphthalene, and it provided a convenient way to assign provisional conformations and population distributions to the mixture of atropisomers.

Our key goal was to eliminate atropisomeric properties completely. Thus, we modified the 8-membered ring system

of **5** by placing a methyl substituent on each of the four positions of the ethyl segment of the ring (**6–9**) and compared the atropisomeric distributions. As expected, the addition of the methyl group did influence the atropisomeric distribution, and two of the four isomers existed in predominantly a single conformational form. Among these two, **9** was the most potent in our in vivo model for CNS activity.

Starting from the ring system in **9**, we made alterations to the left side region in attempt to further improve activity. In this manner, we identified **13**, which showed excellent potency in the in vivo model and long duration of action. Crystallographic analysis of **17** (a close analogue of **13**) confirmed the structural features which had been predicted from structural analysis and modeling. Based on these results, we propose a binding conformation and NK₁ pharmacophore model which involves an edge-to-face aryl–aryl stacking interaction and a hydrogen bonding acceptor group.

5. Experimental

5.1. Molecular modeling

Molecular mechanics computations were performed in vacuo, using the AESOP²⁰ force field with full geometry optimization of all conformations examined and results were visualized using the in-house molecular graphics program ENIGMA.²⁴

5.2. Biological studies

Isolated tissue response (pK_B), studies were carried out as previously described.²⁵ Inhibition of gerbil foot tapping (GFT) response studies were carried out as previously described.²²

5.3. Drug exposure analysis

Studies were conducted in fed mongolian gerbils. The animals received 100 μmol/kg drug by oral administration in a dosing volume of 6 mL/kg in a 75% PEG400/saline solution. The gerbils were euthanized at 4 h after dosing by CO₂ inhalation and brain tissue samples were collected. Samples were stored at –20 °C or below until analysis. Brain homogenates were prepared in a tissue homogenizer using four milliliters of saline per gram of tissue. Samples were processed for analysis by the addition of acidified acetonitrile. The resulting extracts were analyzed by LC/MS.

5.4. Bioavailability analysis

Compounds were orally administered to rat (*n*=2) as a solution in 75% PEG400/saline solution. Blood samples were taken via surgically implanted cannula or by venipuncture over a 24 h period and plasma was analyzed for unchanged compound by LC/MS.

5.5. General chemistry methods

¹H NMR spectra were obtained at 300 MHz using a Bruker DPX 300 spectrometer and were referenced to TMS unless

otherwise noted. Mass spectral data were obtained on a Micromass QTOF mass spectrometer. Silica gel chromatography was performed with ICN silica 32–63, 60 Å. Thin-layer chromatography was done on silica gel 60 F-254 (0.25 mm thickness) plates, and visualization was accomplished with UV light. Unless otherwise noted, all materials were obtained commercially and used without further purification. For compounds which exist as a mixture of atropisomers, ¹H NMR spectra and HPLC chromatograms are complex. In these cases, ¹H NMR integrations are not given. Mass spectra were acquired using atmospheric pressure chemical ionization. High resolution mass spectra were acquired using electrospray (ES). The synthesis of compounds **3**, **4**, **6**, **7**, **8**, and **9** are described separately.¹⁵

5.5.1. 2-[(2*S*)-2-(3,4-Dichlorophenyl)-4-(diethylamino)butyl]-1-oxo-1,3,4,6-tetrahydro-2*H*-naphtho[1,2-*f*][1,4]-oxazocine-7-carbonitrile (2**).** Aldehyde **3**²⁶ (100 mg, 0.21 mmol) was dissolved in methanol (2 mL) under a nitrogen atmosphere. To this was added diethylamine hydrochloride (35 mg, 0.32 mmol) and triethylamine (34 μL, 0.25 mmol). Acetic acid was added dropwise until the pH was between 4 and 5. The mixture was stirred for 10 min, then 22 mg (0.36 mmol) sodium cyanoborohydride was added as a solution in methanol (approx. 1 mL). After stirring for 1.5 h the pH was adjusted to approximately 5.5 by addition of triethylamine and stirring was continued overnight. The mixture was then concentrated, diluted with ethyl acetate (20 mL), washed with water then brine (20 mL each), dried over magnesium sulfate, filtered and concentrated. The remaining residue was then purified via reverse phase HPLC (using a gradient of acetonitrile in water) to give the title compound (80 mg, 60%) as a gum, δ_H (300 MHz, d₆-DMSO) 9.09 (s), 8.68 (s), 8.62 (s), 8.10 (d, *J*=7.7 Hz), 8.02 (d, *J*=8.2 Hz), 7.90 (d, *J*=8.3 Hz), 7.70 (m), 7.42 (m), 6.44 (d, *J*=8.5 Hz), 4.81 (m), 4.34 (m), 4.00 (t, *J*=11.3 Hz), 3.45 (m), 2.71 (m), 2.08 (s), 1.13 (t, *J*=7.1 Hz); *m/z* (APCI) 524 MH⁺.

5.5.2. 2-[(2*S*)-2-(3,4-Dichlorophenyl)-4-(dimethylamino)butyl]-1-oxo-1,3,4,6-tetrahydro-2*H*-naphtho[1,2-*f*][1,4]oxazocine-7-carbonitrile (5**).** Aldehyde **3**²⁶ (150 mg, 0.32 mmol) was dissolved in methanol (3 mL) under a nitrogen atmosphere. To this was added dimethylamine hydrochloride (40 mg, 0.48 mmol) and triethylamine (50 μL, 0.35 mmol). Acetic acid was added dropwise until the pH was between 4 and 5. The mixture was stirred for 0.5 h, then 34 mg (0.54 mmol) sodium cyanoborohydride was added as a solution in methanol (approx. 1 mL). After stirring for 2 h the mixture was then concentrated, diluted with ethyl acetate (30 mL), washed with water then brine (30 mL each), dried over magnesium sulfate, filtered and concentrated. The remaining residue was then purified silica gel chromatography (6–10% MeOH/CH₂Cl₂) to afford the title product (120 mg, 80%) a white solid, δ_H (300 MHz, d₆-DMSO) 8.68 (s), 8.62 (s), 8.09 (d, *J*=7.8 Hz), 8.01 (d, *J*=8.1 Hz), 7.90 (d, *J*=8.3 Hz), 7.82–7.59 (m), 7.40 (m), 6.43 (d, *J*=8.5 Hz), 4.87 (m), 4.71 (t, *J*=12.0 Hz), 4.32 (m), 3.99 (t, *J*=11.1 Hz), 3.89–3.64 (m), 3.42–2.94 (m), 2.83–2.55 (m), 2.10 (s); *m/z* (APCI) 496 MH⁺.

5.5.3. (4*R*)-2-[(2*S*)-2-(3,4-Dichlorophenyl)-4-(methylamino)butyl]-4-methyl-1-oxo-1,3,4,6-tetrahydro-2*H*-naphtho[1,2-*f*][1,4]oxazocine-7-carbonitrile (10**).** Aldehyde

4¹⁵ (70 mg, 0.145 mmol) was dissolved in 1 mL of THF and methylamine in THF (2 M, 87 μ L, 0.174 mmol) was added. The mixture was diluted with methanol (2 mL), and then acetic acid (5 μ L) was added and the mixture stirred for 10 min. A solution of sodium cyanoborohydride (1 M in THF, 0.5 mL, 0.500 mmol) was added and the reaction was stirred overnight at ambient temperature. The reaction mixture was evaporated and the residue purified by preparative HPLC using a Phenomenex LUNA C-18(2), 250 \times 21.2 mm (10 μ) column eluting with acetonitrile–water gradient containing 0.1% TFA (40–70% acetonitrile over 20 min). Product containing fractions were pooled and partially concentrated to remove acetonitrile. The remaining aqueous solution was made basic by addition of 10% aqueous sodium carbonate, and the solution extracted with ethyl acetate (3 times, 20 mL). The organic extracts were dried (Na₂SO₄), filtered and evaporated to afford the title compound (40 mg, 55%) as a white foamy solid, δ_{H} (300 MHz, d₆-DMSO) 8.66 (s, 1H), 8.30 (1H, br), 8.05 (1H, d, *J*=8.3 Hz), 7.67 (3H, m), 7.42 (2H, m), 6.54 (1H, d, *J*=8.3 Hz), 4.95 (1H, d, *J*=13.8 Hz), 4.71 (1H, m), 4.51 (1H, d, *J*=13.8 Hz), 4.03 (1H, m), 3.24 (1H, m), 2.99–2.53 (6H, m), 2.37 (2H, m), 2.01 (2H, m), 1.10 (3H, d, *J*=6.1 Hz); *m/z* (APCI) 496 MH⁺.

5.5.4. (4R)-2-[(2S)-2-(3,4-Dichlorophenyl)-4-piperidin-1-ylbutyl]-4-methyl-1-oxo-1,3,4,6-tetrahydro-2H-naphtho[1,2-*f*][1,4]oxazocine-7-carbonitrile (11). Aldehyde **4**¹⁵ (70 mg, 0.145 mmol) was dissolved in THF (1 mL) and piperidine (15 mg, 0.176 mmol) was added. The mixture was diluted with methanol (2 mL), then acetic acid (5 μ L) was added and the mixture stirred for 10 min. A solution of sodium cyanoborohydride (1 M in THF, 0.5 mL, 0.500 mmol) was added and the reaction was stirred overnight at ambient temperature. The reaction mixture was evaporated and the residue purified by preparative HPLC according to the procedure described for **10** to afford of the title compound as a white foamy solid (50 mg, 62%), δ_{H} (300 MHz, d₆-DMSO) 8.68 (1H, s), 8.39 (1H, br), 8.04 (1H, d, *J*=7.9 Hz), 7.68 (3H, m), 7.43 (2H, m), 6.55 (1H, d, *J*=8.3 Hz), 4.96 (1H, d, *J*=13.8 Hz), 4.72 (1H, m), 4.51 (1H, d, *J*=13.8 Hz), 4.04 (1H, m), 3.02–2.52 (8H, m), 2.05 (2H, m), 1.09 (3H, d, *J*=6.6 Hz), 0.96 (1H, m), 0.55 (2H, m), 0.30 (2H, m); *m/z* (APCI) 550 MH⁺; HRMS (ES) M⁺, found 550.2007. C₃₁H₃₃Cl₂N₃O₂ requires 550.2028.

5.5.5. (4R)-2-[(2S)-4-(tert-Butylamino)-2-(3,4-dichlorophenyl)butyl]-4-methyl-1-oxo-1,3,4,6-tetrahydro-2H-naphtho[1,2-*f*][1,4]oxazocine-7-carbonitrile (12). Aldehyde **4**¹⁵ (70 mg, 0.145 mmol) was dissolved THF (1 mL) and *tert*-butylamine (13 mg, 0.177 mmol) was added. The mixture was diluted with methanol (2 mL), then acetic acid (5 μ L) was added and the mixture stirred for 10 min. A solution of sodium cyanoborohydride (1 M in THF, 0.5 mL, 0.500 mmol) was added and the reaction was stirred overnight at ambient temperature. The reaction mixture was evaporated and the residue purified by preparative HPLC according to the procedure described for **10** to afford the title compound as a white foamy solid (50 mg, 64%), δ_{H} (300 MHz, d₆-DMSO) 8.67 (1H, s), 8.27 (1H, br), 8.05 (1H, d, *J*=8.3 Hz), 7.72–7.64 (3H, m), 7.43 (2H, m), 6.60 (1H, d, *J*=8.7 Hz), 4.96 (1H, d, *J*=14.0 Hz), 4.73 (1H, m), 4.52 (1H, d, *J*=14.0 Hz), 4.05 (1H, m), 2.94 (3H, m), 2.75–2.53 (3H, m), 2.02 (2H, m), 1.21 (9H, s), 1.10 (3H, d, *J*=6.5 Hz);

m/z (APCI) 538 MH⁺; HRMS (ES) M⁺, found 538.2051. C₃₀H₃₃Cl₂N₃O₂ requires 538.2028.

5.5.6. (4R)-2-[(2S)-2-(3,4-Dichlorophenyl)-4-(methoxyamino)butyl]-4-methyl-1-oxo-1,3,4,6-tetrahydro-2H-naphtho[1,2-*f*][1,4]oxazocine-7-carbonitrile (13). Aldehyde **4**¹⁵ (70 mg, 0.145 mmol) was dissolved THF (1 mL) and *O*-methylhydroxylamine hydrochloride (14 mg, 0.167 mmol) was added. The mixture was diluted with methanol (2 mL), then acetic acid (5 μ L) was added and the mixture stirred for 10 min. A solution of sodium cyanoborohydride (1 M in THF, 0.5 mL, 0.500 mmol) was added and the reaction was stirred overnight at ambient temperature. The reaction mixture was evaporated and the residue purified by preparative HPLC according to the procedure described for **10** to afford the title compound as a white foamy solid (21 mg, 28%), δ_{H} (300 MHz, CDCl₃) 8.25 (1H, s), 8.81 (1H, d, *J*=7.4 Hz), 7.60–7.46 (3H, m), 7.39 (1H, d, *J*=1.7 Hz), 7.31–7.25 (1H, m), 6.68 (1H, d, *J*=8.3 Hz), 5.53 (1H, br), 5.14 (1H, d, *J*=13.6 Hz), 4.02 (1H, t, *J*=13.7 Hz), 4.56 (1H, d, *J*=13.7 Hz), 3.96 (1H, m), 3.52 (3H, s), 3.24–3.02 (4H, m), 2.80 (2H, m), 1.96 (2H, m), 1.17 (3H, d, *J*=6.6 Hz); *m/z* (APCI) 512 MH⁺; HRMS (ES) M⁺, found 512.1343. C₂₇H₂₇Cl₂N₃O₃ requires 512.1508.

5.5.7. (4R)-2-[(2S)-2-(3,4-Dichlorophenyl)-4-hydroxybutyl]-4-methyl-1-oxo-1,3,4,6-tetrahydro-2H-naphtho[1,2-*f*][1,4]oxazocine-7-carbonitrile (14). Aldehyde **4**¹⁵ (250 mg, 0.52 mmol) was dissolved in methanol (5 mL) under a nitrogen atmosphere and cooled to 5 °C. Sodium borohydride (22 mg, 0.57 mmol) was then added, the cooling bath removed, and the reaction allowed to stir for 15 min. It was then concentrated, diluted with ethyl acetate, washed with water then brine, dried over magnesium sulfate, filtered and concentrated. The residue was then purified via silica gel chromatography (60–80% ethyl acetate/hexanes) to give the title compound as a foamy solid (200 mg, 80%), δ_{H} (300 MHz, CDCl₃) 8.25 (1H, s), 7.82 (1H, d, *J*=7.7 Hz), 7.54 (3H, m), 7.41 (1H, d, *J*=2.0 Hz), 7.29 (1H, m), 6.69 (1H, d, *J*=8.3 Hz), 5.15 (1H, d, *J*=13.8 Hz), 4.94 (1H, t, *J*=12.4 Hz), 4.57 (1H, d, *J*=13.8 Hz), 3.96 (1H, m), 3.70 (1H, m), 3.47 (1H, m), 3.29 (2H, m), 3.14 (3H, m), 1.98 (2H, m), 1.17 (3H, d, *J*=6.5 Hz); *m/z* (APCI) 438 MH⁺; HRMS (ES) M⁺, found 483.1223. C₂₆H₂₄Cl₂N₂O₃ requires 483.1242.

5.5.8. (4R)-2-[(2S)-4-Chloro-2-(3,4-dichlorophenyl)butyl]-4-methyl-1-oxo-1,3,4,6-tetrahydro-2H-naphtho[1,2-*f*][1,4]oxazocine-7-carbonitrile (15). Alcohol **14** (80 mg, 0.17 mmol) was dissolved in toluene (3.5 mL) under a nitrogen atmosphere and to this was added triphenylphosphine (48 mg, 0.18 mmol), then hexachloroacetone (264 mg, 0.42 mmol) over one min. as a solution in toluene. The reaction was allowed to stir for 1 h, heated briefly to 60 °C, cooled and allowed to stir overnight at room temperature. A second portion of triphenylphosphine (10 mg) and hexachloroacetone (2 drops) were added and reaction again heated briefly to 60 °C, cooled, then concentrated. The remaining residue was purified via silica gel chromatography (30–40% ethyl acetate/hexanes) to give the title compound as a foam solid (80 mg, 96%), δ_{H} (300 MHz, CDCl₃) 8.26 (1H, s), 7.83 (1H, d, *J*=7.8 Hz), 7.54 (3H, m), 7.43 (1H, d, *J*=2.0 Hz), 7.28 (1H, m), 6.73 (1H, d, *J*=8.4 Hz), 5.17 (1H, d,

$J=13.8$ Hz), 4.95 (1H, t, $J=12.2$ Hz), 4.58 (1H, d, $J=13.8$ Hz), 3.99 (1H, m), 3.60 (1H, m), 3.23 (5H, m), 2.18 (2H, m), 1.19 (3H, d, $J=6.5$ Hz); m/z (APCI) 501 MH^+ ; HRMS (ES) M^+ , found 501.0905. $C_{26}H_{23}Cl_3N_2O_2$ requires 501.0903.

5.5.9. (3S)-4-[(4R)-7-Cyano-4-methyl-1-oxo-1,3,4,6-tetrahydro-2H-naphtho[1,2-f][1,4]oxazocin-2-yl]-3-(3,4-dichlorophenyl)butanoic acid (16). Aldehyde **4**¹⁵ (850 mg, 1.77 mmol) was dissolved in acetone (10 mL) under a nitrogen atmosphere and cooled to 0 °C. Jones reagent (2 M, 1.3 mL, 2.65 mmol) was added as a solution in acetone (4 mL) over 5 min. The reaction was stirred for 5 min, then 2-propanol (3 mL) was added and stirred for 5 min. The mixture was concentrated, diluted with ethyl acetate (15 mL), washed with water then brine (15 mL each), dried over magnesium sulfate, filtered and concentrated to give the title compound as a foamy solid (850 mg, 97%), δ_H (300 MHz, $CDCl_3$) 8.27 (1H, s), 7.84 (1H, d, $J=7.8$ Hz), 7.55 (3H, m), 7.42 (1H, d, $J=2.0$ Hz), 7.29 (1H, m), 6.67 (1H, d, $J=8.4$ Hz), 5.17 (1H, d, $J=13.9$ Hz), 4.94 (H, t, $J=12.2$ Hz), 4.56 (1H, d, $J=13.9$ Hz), 3.9 (1H, m), 3.51 (1H, m), 3.19 (3H, m), 2.83 (2H, d, $J=7.2$ Hz), 1.20 (3H, d, $J=6.5$ Hz); m/z (APCI) 497 MH^+ ; HRMS (ES) M^+ , found 497.1027. $C_{26}H_{22}Cl_2N_2O_4$ requires 497.1035.

5.5.10. (3S)-4-[(4R)-7-Cyano-4-methyl-1-oxo-1,3,4,6-tetrahydro-2H-naphtho[1,2-f][1,4]oxazocin-2-yl]-3-(3,4-dichlorophenyl)butanamide (17). Carboxylic acid **16** (80 mg, 0.16 mmol) was dissolved in dichloromethane (3 mL) under a nitrogen atmosphere; to this was added diisopropylethylamine (55 μ L, 0.32 mmol), then fluoro-*N,N'*-tetramethylforamidinium hexafluorophosphate (51 mg, 0.19 mmol). After 1 h $HOBt-NH_3$ ²⁷ (43 mg, 0.32 mmol) was added and the mixture stirred for 2 h. Saturated aqueous sodium bicarbonate and ethyl acetate were added (15 mL each) and the mixture was washed with aqueous sodium bicarbonate, then brine (15 mL each), dried over magnesium sulfate and purified via silica gel chromatography (5–7% methanol/methylene chloride) to give the title compound as a foamy solid (60 mg, 76%), δ_H (300 MHz, $CDCl_3$) 8.25 (1H, s), 7.82 (1H, d, $J=7.8$ Hz), 7.52 (4H, m), 7.28 (1H, m), 6.68 (1H, d, $J=8.3$ Hz), 5.43 (2H, m), 5.16 (1H, d, $J=13.9$ Hz), 4.94 (1H, t, $J=12.6$ Hz), 4.56 (1H, d, $J=13.9$ Hz), 3.97 (1H, m), 3.60 (1H, m), 3.26 (1H, m), 3.15 (2H, d, $J=7.1$ Hz), 2.64 (2H, m), 1.19 (3H, d, $J=6.5$ Hz); m/z (APCI) 496 MH^+ ; HRMS (ES) M^+ , found 496.1194. $C_{26}H_{23}Cl_2N_3O_3$ requires 496.1194. Crystals suitable for diffraction were prepared by dissolving the compound in ethyl acetate/methylene chloride (10:1) and allowing diethyl ether to diffuse into the solution in a closed vial, mp 168–170 °C, $[\alpha]_D^{20}=-130$ (c 0.5, methanol). Crystallographic data (excluding structure factors) for the structure in this paper was deposited with the Cambridge Crystallographic Data Center as supplementary publication numbers CCDC 230503. Copies of the data can be obtained, free of charge, on application to CCDC, 12 Union Road, Cambridge CB2 1EZ, UK [fax: 144-(0)1223-336033 or e-mail: deposit@ccdc.cam.ac.uk].

5.5.11. (3S)-4-[(4R)-7-Cyano-4-methyl-1-oxo-1,3,4,6-tetrahydro-2H-naphtho[1,2-f][1,4]oxazocin-2-yl]-3-(3,4-

dichlorophenyl)-*N*-methylbutanamide (18). Carboxylic acid **16** (80 mg, 0.16 mmol) was dissolved in dichloromethane (2 mL) under a nitrogen atmosphere; to this was added oxalyl chloride (28 μ L, 0.32 mmol) and one drop of dimethylformamide. After stirring for 0.5 h, the mixture was concentrated, redissolved in dichloromethane (1 mL) and concentrated again. The residue was dissolved in dichloromethane (2 mL) and to this was added methylamine (2 M solution in THF, 120 μ L, 0.24 mmol), and triethylamine (32 μ L, 0.24 mmol). The mixture was stirred for 1 h, concentrated and purified using reverse phase HPLC to give the title compound as a white solid (60 mg, 60%), δ_H (300 MHz, $CDCl_3$) 8.26 (1H, s), 7.83 (1H, d, $J=7.8$ Hz), 7.53 (4H, m), 7.26 (1H, m), 6.67 (1H, d, $J=8.4$ Hz), 5.74 (1H, d, $J=4.1$ Hz), 5.16 (1H, m), 4.93 (1H, m), 4.56 (1H, m), 3.98 (1H, m), 3.65 (1H, m), 3.27 (1H, m), 3.12 (2H, m), 2.78 (d, $J=4.8$ Hz), 2.62 (2H, m), 1.18 (3H, d, $J=6.5$ Hz); m/z (APCI) 510 MH^+ ; HRMS (ES) M^+ , found 510.1356. $C_{27}H_{25}Cl_2N_3O_3$ requires 510.1351.

5.5.12. (3S)-4-[(4R)-7-Cyano-4-methyl-1-oxo-1,3,4,6-tetrahydro-2H-naphtho[1,2-f][1,4]oxazocin-2-yl]-3-(3,4-dichlorophenyl)-*N,N*-dimethylbutanamide (19). Carboxylic acid **16** (80 mg, 0.16 mmol) was dissolved in dichloromethane (2 mL) under a nitrogen atmosphere; to this was added oxalyl chloride (28 μ L, 0.32 mmol) and one small drop of dimethylformamide. After stirring for 0.5 h, the mixture was concentrated, redissolved in dichloromethane (1 mL) and concentrated again. The residue was dissolved in dichloromethane (2 mL) and to this was added dimethylamine (120 μ L of 2 M solution in tetrahydrofuran, 0.24 mmol), and triethylamine (32 μ L, 0.24 mmol). The mixture was stirred for 15 min, concentrated and purified using silica gel chromatography (2–3% methanol/dichloromethane) to give the title compound as a foamy solid (80 mg, 95%), δ_H (300 MHz, $CDCl_3$) 8.24 (1H, s), 7.81 (1H, d, $J=7.8$ Hz), 7.51 (4H, m), 7.30 (1H, m), 6.62 (1H, d, $J=8.3$ Hz), 5.15 (1H, d, $J=13.8$ Hz), 4.92 (1H, t, $J=12.6$ Hz), 4.56 (1H, d, $J=13.8$ Hz), 4.00 (1H, m), 3.64 (1H, m), 3.31 (2H, m), 3.11 (1H, m), 3.00 (3H, s), 2.95 (3H, s), 2.70 (2H, d, $J=6.7$ Hz), 1.22 (3H, d, $J=6.5$ Hz); m/z (APCI) 524 MH^+ ; HRMS (ES) M^+ , found 524.1501. $C_{28}H_{27}Cl_2N_3O_3$ requires 524.1508.

References and notes

1. Stout, S. C.; Owens, M. J.; Nemeroff, C. B. *Annu. Rev. Pharmacol. Toxicol.* **2001**, *41*, 877–906.
2. Chahl, L. A.; Urban, L. A. *Pharmacol. Rev. Commun.* **1999**, *10*, 197–203.
3. Swain, C.; Rupniak, N. M. *J. Annu. Rep. Med. Chem.* **1999**, *34*, 51–60.
4. Gerspacher, M.; Von Sprecher, A. *Drugs Future* **1999**, *24*, 883–892.
5. Gao, Z.; Peet, N. P. *Curr. Med. Chem.* **1999**, *6*, 375–388.
6. Sakurada, T.; Sakurada, C.; Tan-No, K.; Kisara, K. *CNS Drugs* **1997**, *8*, 436–447.
7. Snider, R. M.; Constantine, J. W.; Lowe, J. A., III; Longo, K. P.; Lebel, W. S.; Woody, H. A.; Drozda, S. E.; Desai, M. C.; Vinick, F. J.; Science, F. J. *Science* **1991**, *251*, 435–437.
8. Emonds-Alt, X.; Proietto, V.; Van Broeck, D.; Vilain, P.;

- Advenier, C.; Neliat, G.; Le Fur, G.; Brellere, J. C. *Bioorg. Med. Chem. Lett.* **1993**, *3*, 925–930.
9. Albert, J. S.; Aharony, D.; Andisik, D.; Barthlow, H.; Bernstein, P. R.; Bialecki, R. A.; Dedinas, R.; Dembofsky, B. T.; Hill, D.; Kirkland, K.; Koether, G. M.; Kosmider, B. J.; Ohnmacht, C.; Palmer, W.; Potts, W.; Rumsey, W.; Shen, L.; Shenvi, A.; Sherwood, S.; Warwick, P. J.; Russell, K. *J. Med. Chem.* **2002**, *45*, 3972–3983.
10. Albert, J. S.; Ohnmacht, C.; Bernstein, P. R.; Rumsey, W. L.; Aharony, D.; Alelyunas, Y.; Russell, D. J.; Potts, W.; Sherwood, S. A.; Shen, L.; Dedinas, R. F.; Palmer, W. E.; Abbott, B. M.; Russell, K. *J. Org. Chem.* **2004**, *47*, 519–529.
11. Clayden, J.; Pink, J. H. *Angew. Chem., Int. Ed.* **1998**, *37*, 1937–1939.
12. Ahmed, A.; Bragg, R. A.; Clayden, J.; Lai, L. W.; McCarthy, C.; Pink, J. H.; Westlund, N.; Yasin, S. A. *Tetrahedron* **1998**, *54*, 13277–13294.
13. Iwamura, H.; Mislow, K. *Acc. Chem. Res.* **1988**, *21*, 175–182.
14. Natsugari, H.; Ikeura, Y.; Kamo, I.; Ishimaru, T.; Ishichi, Y.; Fujishima, A.; Tanaka, T.; Kasahara, F.; Kawada, M.; Doi, T. *J. Med. Chem.* **1999**, *42*, 3982–3993.
15. Ohnmacht, C. J.; Albert, J. S.; Bernstein, P. R.; Rumsey, W. L.; Masek, B. B.; Dembofsky, B. T.; Koether, G. M.; Andisik, D. W.; Aharony, D. *Bioorg. Med. Chem.* **2004**, *12*, see doi: 10.1016/j.bmc.2004.03.015.
16. Anet, F. A. L.; Yavari, I. *Tetrahedron* **1978**, *34*, 2879–2886.
17. Anet, F. A. L.; Yavari, I. *J. Am. Chem. Soc.* **1978**, *100*, 7814–7819.
18. Burkert, U.; Allinger, N. L. *Molecular mechanics*; American Chemical Society: Washington, DC, 1982.
19. Sandstrom, J. *Dynamic NMR spectroscopy*; Academic: New York, 1982.
20. AESOP is an in-house molecular mechanics program (Masek, B.) derived from BIGSTRN-3 (QCPE-514) Nachbar, R., Jr.; Mislow, K. *QCPE Bull.* **1986**, *6*, 96.
21. Bernstein, P. R.; Aharony, D.; Albert, J. S.; Andisik, D.; Barthlow, H. G.; Bialecki, R.; Davenport, T.; Dedinas, R. F.; Dembofsky, B. T.; Koether, G.; Kosmider, B. J.; Kirkland, K.; Ohnmacht, C. J.; Potts, W.; Rumsey, W. L.; Shen, L.; Shenvi, A.; Sherwood, S.; Stollman, D.; Russell, K. *Bioorg. Med. Chem. Lett.* **2001**, *11*, 2769–2773.
22. Rupniak, N. M. J.; Tattersall, F. D.; Williams, A. R.; Rycroft, W.; Carlson, E. J.; Cascieri, M. A.; Sadowski, S.; Ber, E.; Hale, J. J.; Mills, S. G.; MacCoss, M.; Seward, E.; Huscroft, I.; Owen, S.; Swain, C. J.; Hill, R. G.; Hargreaves, R. J. *Eur. J. Pharmacol.* **1997**, *326*, 201–209.
23. Drug exposure is expressed in terms of amount of drug (ng) per unit of brain tissue (g) 4 h following oral dosing at the indicated quantity; see Section 5.
24. ENIGMA is an in-house molecular graphics program.
25. Rumsey, W. L.; Aharony, D.; Bialecki, R. A.; Abbott, B. M.; Barthlow, H. G.; Caccese, R.; Ghanekar, S.; Lengel, D.; McCarthy, M.; Wenrich, B.; Udem, B.; Ohnmacht, C.; Shenvi, A.; Albert, J. S.; Brown, F.; Bernstein, P. R.; Russell, K. *J. Pharmacol. Exp. Ther.* **2001**, *298*, 307–315.
26. Manuscript in preparation.
27. Bajusz, S.; Ronai, A. Z.; Szekely, J. I.; Graf, L.; Dunai-Kovacs, Z.; Berzetei, I. *FEBS Lett.* **1977**, *76*, 91–92.